Composite Structures 115 (2014) 111–119

Contents lists available at ScienceDirect

Composite Structures

journal homepage: www.elsevier.com/locate/compstruct

Effective properties of elastic composite materials with multi-coated reinforcements: A new micromechanical modelling and applications

Napo Bonfoh *, Mamadou Coulibaly, Hafid Sabar

Laboratoire de Mécanique Biomécanique Polymère Structures, Ecole Nationale d'Ingénieurs de Metz, 1 route d'Ars Laquenexy, 57078 Metz, France

A R T I C L E   I N F O

Article history:
Available online 30 April 2014

Keywords:
Composite materials
Interphase
Micromechanics
Multi-coated inclusion
Generalized Self-Consistent Scheme

A B S T R A C T

In this work, a homogenisation method for the prediction of the effective properties of composite materials with multi-coated reinforcements is presented. Based on Green's function techniques as well as interior and exterior-point Eshelby tensors for an ellipsoidal inclusion embedded in an infinite medium, a new micromechanical approach applied to the multi-coated inclusion problem is developed. The case of multi-coated spherical inclusion and isotropic materials is presented in order to provide analytical expressions of the local strains and stresses through concentration equations. Using Generalized Self-Consistent Scheme, the effective elastic properties of homothetic particle-reinforced materials are obtained. The model is applied to three-phase materials and results are compared to exact analytical solutions. The results are also presented regarding the influence of the interphase on the effective moduli and compared with those of other models including numerical investigations.

1. Introduction

Over the last few decades, the use of composite materials has significantly increased and become widespread. Indeed, by judicious combinations, this type of materials can reach high performances while remaining light weight. Generally, these materials consist of a continuous phase (matrix) into which reinforcements (inclusions) of one or several phases are distributed randomly or periodically. Due to heterogeneous nature of composite materials, their mechanical properties depend on component characteristics and spatial distribution. The use of an adapted scale transition method allows to establish a relation between local and effective properties of these materials.

As is evident from the experimental observations, producing composite materials involves the presence of an interphase layer surrounding the reinforcements. In some configurations, the layer, considering as a different phase, results from sizing [1], chemical reaction between the reinforcements and the matrix [2] or diffusion process [3] during the manufacturing of the composite material. Otherwise, the layer is a thin interphase introduced to protect the reinforcement or to insure a better adhesion at matrix-reinforcement interface. Due to its major role in the load transfer between the reinforcements and the matrix, the interphase layer has a significant effect on local stress fields and effective properties of the composite material. Consequently, a rigorous evaluation of these effective properties might take into account the mechanical characteristics of this interphase.

Using mean-field homogenisation schemes, micromechanical models predict the overall properties of composite materials from the constituent characteristics (reinforcement, interphase and matrix) and the microstructural morphology of a representative volume element (RVE). From the inclusion problem of Eshelby [4], the different models address the coated inclusion problem by considering an inclusion surrounded by a layer (interphase) and its corresponding composite inclusion embedded in an infinite matrix. According to Eshelby's model, the strain field inside an ellipsoidal inclusion is uniform and the infinite matrix undergoes uniform strain at infinity. Thanks to these conditions, analytical expressions of mechanical responses are implemented in the general framework of composite materials, providing a valuable tool for research and development. In the coated inclusion consideration, the presence of the interphase has a disturbing effect on the strain fields inside the inclusion. Furthermore, due to complex inclusion-interphase and interphase-matrix interactions, the local strain fields are heterogeneous inside both interphase and inclusion. Generally, the solution of the coated inclusion problem remains a arduous achievement. To deal with this challenging problem, most existing micromechanical models are developed using two main approaches.

On the one hand, a first approach is based on the displacement potentials method of Papkovich–Neuber, which provides the general solution of fundamental differential equations in elasticity. This solution is expressed in terms of the spherical harmonic

* Corresponding author. Tel.: +33 (0) 3 87 79 68 16; fax: +33 (0) 3 87 34 42 78.
E-mail address: bonfoh@enim.fr (N. Bonfoh).

http://dx.doi.org/10.1016/j.compstruct.2014.04.011
0263-8223/

functions. In the cases of spherical or cylindrical symmetry, exact analytical expressions of the displacements and local stresses have been formalised by Love [5]. This exact approach was used to treat the coated-inclusion problem with spherical or cylindrical homothetic and concentric inclusions. Some notable resulting micromechanical contributions are the composite sphere assembly model [6], the generalized self-consistent model [7], the n-layered spherical inclusion model [8] and n-layered cylindrical inclusion model [9]. From the latter reference models, other investigations were also achieved to study the interphase influence on the effective behaviour of composite materials [10–17]. In spite of the relevance of these micromechanical models, applications remain limited to the cases of the spherical or cylindrical inclusions, isotropic or transversally isotropic elasticity and some specific loadings.

On the second hand, another class of approaches deals with the Green function's techniques, which leads to a Lippmann–Schwinger type integral equation from the field equations of the heterogeneous elastic problem. Among these models, Hori and Nemat–Nasser's double inclusion one [18] gives the solution of the coated-inclusion problem in the case of ellipsoidal inclusions and anisotropic behaviour. However, this model assumes the uniformity of the strain field inside the coating, so that interactions between local phases are partially taken into account and obtained results are then different from the exact solution [8]. Within this framework, another model was also developed in the case of ellipsoidal inclusions and for anisotropic media by introducing the concept of interfacial operators for very thin coatings [19,20]. The resulting solution is relevant only in the particular case of an interphase with a small thickness.

Recently, an approach proposed by Bonfoh et al. [21] is based on the concept of interior and exterior-point Eshelby tensors for an ellipsoidal inclusion embedded in an infinite matrix. The integral equation is solved without simplifying assumptions and analytical obtained results are compared with the exact solution in the case of a coated spherical inclusion in an isotropic infinite medium.

In this paper, the general formulation of multi-coated inclusion problem is proposed in a first part, by considering n-phase multi-coated ellipsoidal inclusion. The second part of this work focuses on the application of the proposed model in the case of an inclusion coated with two layers. Analytical results coincide with the exact solution of Hervé and Zaoui [8]. The third section is devoted to the evaluation of the effective properties of composite materials with doubly coated reinforcements, using the Generalized Self-Consistent Scheme (GSCS). Predictions of the proposed model are compared with numerical results issued from finite-element method (FEM). The developed model is then applied to a three-phase material in order to analyse the effects of the interphase on the effective properties of composite material.

2. Micromechanical model

Fig. 1 shows the topology of the multi-coated inclusion problem, in which an n-phase multi-coated composite inclusion of volume Ω_n is embedded in an infinite reference medium denoted '0'. The so-called 'composite inclusion' consists of an inclusion of volume $V_1 = \Omega_1$ surrounded by $n-1$ coating layers with volume V_k ($k = 2,\dots,n$). Each phase 'k' ($k = 1,\dots,n$) has a linear elastic behaviour described by moduli $\boldsymbol{C}^k$, while the reference medium '0' designates a additional phase characterised by $\boldsymbol{C}^0$. In the present analysis, we assume small deformations and perfect interfaces between the different phases.

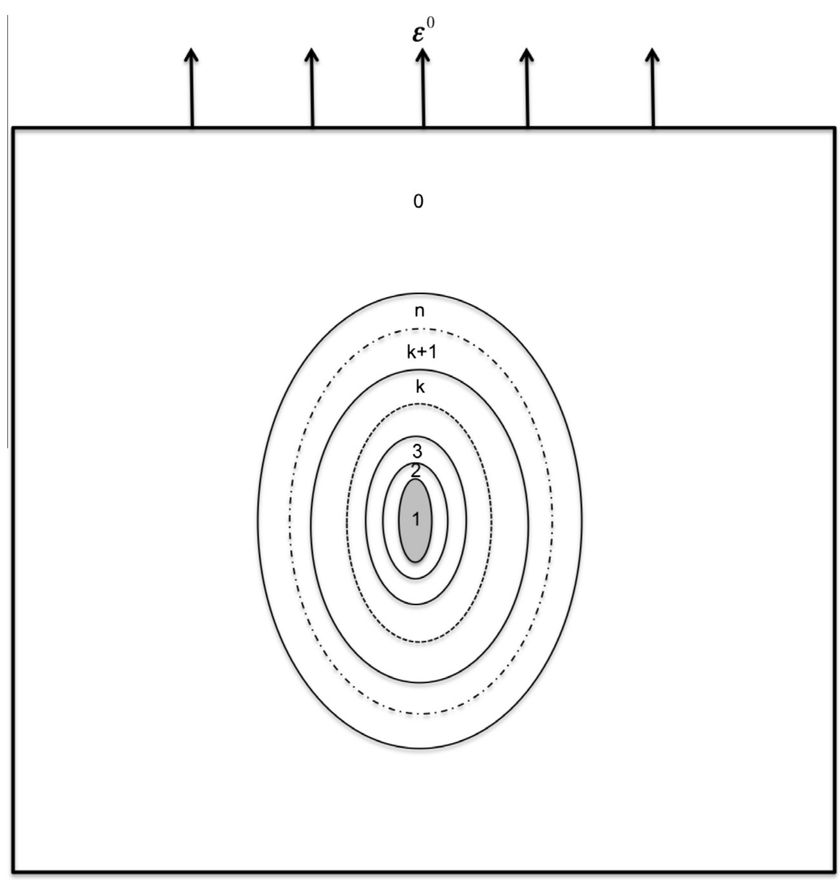

Fig. 1. Topology of the multi-coated inclusion problem.

2.1. Integral equation

Let us consider an elastic heterogeneous medium with the volume V and local elastic moduli $\boldsymbol{C}(\boldsymbol{r})$ and subjected to homogeneous boundary conditions $u_i^0(\boldsymbol{r}) = \varepsilon_{ij}^0 x_j$. Here, $\boldsymbol{\varepsilon}^0$ is a uniform strain imposed on the boundary ∂V of V. Solving the problem thus consists, on the one hand, in determining displacements $u_i(\boldsymbol{r})$, strains $\varepsilon_{ij}(\boldsymbol{r})$ and stresses $\sigma_{ij}(\boldsymbol{r})$ fields of an arbitrary point $\boldsymbol{r}$ (x_1,x_2,x_3) in the volume V, and on the other hand, in estimating the effective properties of the RVE through the homogenisation step.

The field equations of such a heterogeneous problem read as:

- Constitutive law

$$\sigma_{ij}(\boldsymbol{r}) = C_{ijpq}(\boldsymbol{r})\varepsilon_{pq}(\boldsymbol{r}) \tag{1}$$

- Quasi-static equilibrium conditions:

$$\sigma_{ij,j}(\boldsymbol{r}) = 0 \tag{2}$$

- Compatibility relations:

$$\varepsilon_{ij}(\boldsymbol{r}) = \frac{1}{2}(u_{i,j}(\boldsymbol{r}) + u_{j,i}(\boldsymbol{r})) \tag{3}$$

- Kinematic boundary conditions:

$$u_i^0(\boldsymbol{r}) = \varepsilon_{ij}^0 x_j \tag{4}$$

Local moduli $\boldsymbol{C}$ $(\boldsymbol{r})$ is decomposed into the uniform tensor $\boldsymbol{C}^{\boldsymbol{0}}$ corresponding to the reference medium and fluctuations $\delta\boldsymbol{C}$ $(\boldsymbol{r})$ as

$$C_{ijpq}(\boldsymbol{r}) = C_{ijpq}^0 + \delta C_{ijpq}(\boldsymbol{r}) \tag{5}$$

Using the Green's function techniques, an integral equation deduced from Eqs. (1)–(5) links the local displacements $\boldsymbol{u}(\boldsymbol{r})$ with the imposed field $\boldsymbol{u}^{\boldsymbol{0}}$ $(\boldsymbol{r})$ as proposed by Dederichs and Zeller [22] and Kröner [23]:

$$u_i(\boldsymbol{r}) = u_i^0(\boldsymbol{r}) + \int_{V'} G_{ip,q}(\boldsymbol{r}-\boldsymbol{r}')\delta C_{pquv}(\boldsymbol{r}')\,\varepsilon_{uv}(\boldsymbol{r}')dV' \tag{6}$$

where $\boldsymbol{G}$ is the Green's tensor of the reference medium $\boldsymbol{C}^{\boldsymbol{0}}$.

From Eq. (3), the strain field is determined:

$$\varepsilon_{ij}(\boldsymbol{r}) = \varepsilon_{ij}^0 - \int_{V'} \Gamma_{ijpq}(\boldsymbol{r}-\boldsymbol{r}')\,\delta C_{pquv}(\boldsymbol{r}')\,\varepsilon_{uv}(\boldsymbol{r}')dV' \tag{7}$$

where $\boldsymbol{\Gamma}$ is the modified Green tensor:

$$\Gamma_{ijpq}(\boldsymbol{r}-\boldsymbol{r}') = -\frac{1}{2}(G_{ip,qj}(\boldsymbol{r}-\boldsymbol{r}') + G_{jp,qi}(\boldsymbol{r}-\boldsymbol{r}')) \tag{8}$$

The first order spatial variations $\delta\boldsymbol{C}$ $(\boldsymbol{r})$ of the elastic properties are expressed as

$$\delta C_{ijpq}(\boldsymbol{r}) = \sum_{k=1}^{n}\Delta C_{ijpq}^k\theta^k(\boldsymbol{r}) \quad \text{with } \Delta C_{ijpq}^k = C_{ijpq}^k - C_{ijpq}^0 \tag{9}$$

where the characteristic function θ^k $(\boldsymbol{r})$ of the phase k occupying the volume V_k is

$$\theta^k(\boldsymbol{r}) = \begin{cases} 1, & \text{if } \boldsymbol{r} \in V_k \\ 0, & \text{if } \boldsymbol{r} \notin V_k \end{cases} \quad \text{for } k = 1,2,\ldots,n \tag{10}$$

In the following, the composite inclusion of volume Ω_n consists of the inclusion '*1*' and the $n-1$ coatings. For each level '*J*', Ω_J denotes the volume of the composite inclusion which is made up of the inclusion '*1*' and the $J-1$ coatings. ϕ_k represents the volume fraction of phase '*k*' in the composite inclusion Ω_n:

$$\Omega_n = \sum_{k=1}^{n}V_k, \quad \Omega_J = \sum_{k=1}^{J}V_k, \quad \phi_k = \frac{V_k}{\Omega_n} \quad \text{for } k = 1,2,\ldots,n \tag{11}$$

Averaging a field F $(\boldsymbol{r})$ (strain or stress) over volumes V_k and Ω_J respectively yields

$$F^k = \frac{1}{V_k}\int_{V_k}F(\boldsymbol{r})dV, \quad F^{\Omega_J} = \frac{1}{\Omega_J}\int_{\Omega_J}F(\boldsymbol{r})dV \tag{12}$$

Substituting Eq. (9) in Eq. (7) and using function $\theta^k(\boldsymbol{r})$ in Eq. (10) lead to

$$\varepsilon_{ij}(\boldsymbol{r}) = \varepsilon_{ij}^0 - \sum_{k=1}^{n}\int_{V_k'}\Gamma_{ijpq}(\boldsymbol{r}-\boldsymbol{r}')\Delta C_{pquv}^k\varepsilon_{uv}(\boldsymbol{r}')dV' \tag{13}$$

It should be noted that determining field $\boldsymbol{\varepsilon}(\boldsymbol{r})$ at each position $\boldsymbol{r}$ implies complicated evaluation. Therefore, for the sake of simplicity, $\boldsymbol{C}(\boldsymbol{r})$ being uniform in each phase, we reasonably consider averaged strain field. Accordingly, expression of the average strain field ε^{Ω_J} over the composite inclusion Ω_J ($J = 1,2,\ldots,n$) is obtained from Eqs. (12) and (13):

$$\varepsilon_{ij}^{\Omega_J} = \varepsilon_{ij}^0 - \frac{1}{\Omega_J}\sum_{k=1}^{n}\int_{\Omega_J}\int_{V_k'}\Gamma_{ijpq}(\boldsymbol{r}-\boldsymbol{r}')\Delta C_{pquv}^k\varepsilon_{uv}(\boldsymbol{r}')dV'dV \tag{14}$$

In Eq. (14), the Eshelby tensor associated to the composite inclusion Ω_J reads as

$$T_{ijpq}^J(r') = \int_{\Omega_J}\Gamma_{ijpq}(\boldsymbol{r}-\boldsymbol{r}')dV \quad \text{for } \boldsymbol{r}' \in V_k \tag{15}$$

From Eq. (15), the Eshelby tensor depends on the position $\boldsymbol{r}'$ in the phase V_k. Eq. (14) is thus rewritten as

$$\varepsilon_{ij}^{\Omega_J} = \varepsilon_{ij}^0 - \frac{1}{\Omega_J}\sum_{k=1}^{n}\int_{V_k'}T_{ijpq}^J(\boldsymbol{r}')\Delta C_{pquv}^k\varepsilon_{uv}(\boldsymbol{r}')dV' \tag{16}$$

2.2. Solution of the multi-coated inclusion problem

As Eshelby tensor $\boldsymbol{T}^{\boldsymbol{J}}(\boldsymbol{r})$ is uniform inside an ellipsoidal inclusion Ω_J and non-uniform outside, the integral term in Eq. (16) can be evaluated by considering two configurations:

– for $\boldsymbol{r}' \in \Omega_J$, $\boldsymbol{T}^{\boldsymbol{J}}(\boldsymbol{r}')$ corresponds to the interior-point Eshelby tensor $\boldsymbol{T}^{\boldsymbol{Int/J}}$ [4]:

$$T_{ijpq}^{Int/J} = \int_{\Omega_J}\Gamma_{ijpq}(\boldsymbol{r}-\boldsymbol{r}')dV \quad \text{for } \boldsymbol{r}' \in \Omega_J \tag{17}$$

– for $\boldsymbol{r}' \notin \Omega_J$, $\boldsymbol{T}^{\boldsymbol{J}}(\boldsymbol{r}')$ depends on the position $\boldsymbol{r}'$ and corresponds to the exterior-point Eshelby tensor $\boldsymbol{T}^{\boldsymbol{Ext/J}}(\boldsymbol{r}')$ [24]:

$$T_{ijpq}^{Ext/J}(\boldsymbol{r}') = \int_{\Omega_J}\Gamma_{ijpq}(\boldsymbol{r}-\boldsymbol{r}')dV \quad \text{for } \boldsymbol{r}' \notin \Omega_J \tag{18}$$

Thus, Eq. (16) becomes:

$$\varepsilon_{ij}^{\Omega_J} = \varepsilon_{ij}^0 - \frac{\Omega_n}{\Omega_J}\sum_{k=1}^{J}\phi_k T_{ijpq}^{Int/J}\Delta C_{pquv}^k\varepsilon_{uv}^k - \frac{1}{\Omega_J}\sum_{k=J+1}^{n}\int_{V_k'}T_{ijpq}^{Ext/J}(\boldsymbol{r}')\Delta C_{pquv}^k\varepsilon_{uv}(\boldsymbol{r}')dV' \tag{19}$$

Due to the non-uniformity of $\boldsymbol{T}^{\boldsymbol{J}}(\boldsymbol{r}')$ outside Ω_J and the strong interactions between phases of the multi-coated inclusion, the local strain field $\boldsymbol{\varepsilon}(\boldsymbol{r}')$ is also non-uniform inside each phase V_k ($k = 2,\ldots,n$). From the latter fact, determining the integral term in Eq. (19) points out the difficulty encountered to solve the multi-coated inclusion problem.

For the sake of simplicity, Eq. (19) is rewritten as

$$\varepsilon_{ij}^{\Omega_J} = \varepsilon_{ij}^0 - \frac{\Omega_n}{\Omega_J}\sum_{k=1}^{J}\phi_k T_{ijpq}^{Int/k}\Delta C_{pquv}^k\varepsilon_{uv}^k - \sum_{k=J+1}^{n}\varepsilon_{ij}^{k/J} \tag{20}$$

with $\varepsilon_{ij}^{k/J} = \frac{1}{\Omega_J}\int_{V_k}T_{ijpq}^{Ext/J}(\boldsymbol{r})\Delta C_{pquv}^k\varepsilon_{uv}(\boldsymbol{r})dV$.

Tensor $\boldsymbol{\varepsilon}^{k/J}$ remains difficult to be evaluated since $\boldsymbol{T}^{Ext/J}(\boldsymbol{r})$ and $\boldsymbol{\varepsilon}(\boldsymbol{r})$ both depend on the position $\boldsymbol{r}$ and are heterogeneous inside each coating layer V_k. The aim of the present study is then about to compute $\boldsymbol{\varepsilon}^{k/J}$ and to provide the exact solution of the multi-coated inclusion problem. In order to test the relevance of the proposed formulation and to determine explicit analytical expressions, the present work is conducted in isotropic elasticity. In this case, the elastic moduli $\boldsymbol{C}^k$ of each phase 'k' ($k = 0,1,\ldots,n$) are decomposed as

$$C^k_{ijpq} = 3\kappa_k J^1_{ijpq} + 2\mu_k J^2_{ijpq} \quad \text{for } k = 0,1,\ldots,n \tag{21}$$

with $\kappa_k = 2\mu_k(1+\nu_k)/(3(1-2\nu_k))$, $J^1_{ijpq} = \delta_{ij}\delta_{pq}/3$, $J^2_{ijpq} = I_{ijpq} - J^1_{ijpq}$ and $I_{ijpq} = (\delta_{ip}\delta_{jq} + \delta_{iq}\delta_{jp})/2$.

μ_k and ν_k are respectively the shear modulus and the Poisson's ratio of the phase 'k'.

For isotropic elasticity case, Green's tensor $\boldsymbol{G}$ is provided by Mura [25]:

$$G_{ij}(\boldsymbol{r}) = \frac{\delta_{ij}}{4\pi\mu_0 r} - \frac{1}{16\pi\mu_0(1-\nu_0)} r_{,ij} \quad \text{with } r = \sqrt{x_i x_i} \tag{22}$$

Using Eqs. (8), (18) and (22), $\boldsymbol{T}^{Ext/J}$ reads as

$$T^{Ext/J}_{ijpq}(\boldsymbol{r}) = -\frac{1}{8\pi\mu_0}\left(\delta_{ip}\varphi^{Ext/J}_{,jq}(\boldsymbol{r}) + \delta_{jp}\varphi^{Ext/J}_{,iq}(\boldsymbol{r}) - \frac{1}{2(1-\nu_0)}\psi^{Ext/J}_{,ijpq}(\boldsymbol{r})\right) \tag{23}$$

$\varphi^{Ext/J}(\boldsymbol{r})$ and $\psi^{Ext/J}(\boldsymbol{r})$ are respectively the harmonic and bi-harmonic potentials outside the composite inclusion Ω_J:

$$\varphi^{Ext/J}(\boldsymbol{r}) = \int_{\Omega_J} \frac{1}{|\boldsymbol{r}-\boldsymbol{r}'|} dV', \quad \psi^{Ext/J}(\boldsymbol{r}) = \int_{\Omega_J} |\boldsymbol{r}-\boldsymbol{r}'| dV' \quad \text{for } \boldsymbol{r} \notin \Omega_J \tag{24}$$

From Eq. (23), $\varepsilon^{k/J}_{ij}$ is obtained:

$$\begin{aligned}\varepsilon^{k/J}_{ij} = &-\frac{1}{8\pi\mu_0\Omega_J}\int_{V_k}(\Delta C^k_{piuv}\varphi^{Ext/J}_{,pj}(\boldsymbol{r}) + \Delta C^k_{qjuv}\varphi^{Ext/J}_{,qi}(\boldsymbol{r}))\varepsilon_{uv}(\boldsymbol{r})dV \\ &+ \frac{1}{16\pi\mu_0(1-\nu_0)\Omega_J}\int_{V_k}\psi^{Ext/J}_{,ijpq}(\boldsymbol{r})\Delta C^k_{pquv}\varepsilon_{uv}(\boldsymbol{r})dV\end{aligned} \tag{25}$$

In the case of an ellipsoidal inclusion, we can express potentials $\varphi^{Ext/J}(\boldsymbol{r})$ and $\psi^{Ext/J}(\boldsymbol{r})$ in terms of elliptic integrals (see [25]). In order to clearly explicit the method, the present work focuses on the particular case of the multi-coated spherical inclusion. As illustrated in Fig. 1, the outer radius of the composite inclusion Ω_J is denoted a_J ($a_0 = 0$ and $a_{n+1} \to \infty$) and harmonic functions $\varphi^{Ext/J}(\boldsymbol{r})$ and $\psi^{Ext/J}(\boldsymbol{r})$ are given by Mura [25]:

$$\varphi^{Ext/J}(\boldsymbol{r}) = \frac{\Omega_J}{r}, \quad \psi^{Ext/J}_{,i}(\boldsymbol{r}) = \frac{\Omega_J}{5}\left(5\frac{x_i}{r} - a_J^2\frac{x_i}{r^3}\right) \tag{26}$$

In the case of concentric and homothetic spherical inclusions, interior-point Eshelby tensors satisfy

$$\boldsymbol{T}^{Int/J}(\boldsymbol{C}^0) = \boldsymbol{T}^{Int/n}(\boldsymbol{C}^0) \quad \text{for } J = 1,2,\ldots,n \tag{27}$$

In addition, in isotropic elasticity, $\boldsymbol{T}^{Int/n}$ is specified by Kröner [26]:

$$T^{Int/n}_{ijpq}(\boldsymbol{C}^0) = \frac{\alpha_0}{3}J^1_{ijpq} + \frac{\beta_0}{2}J^2_{ijpq} \tag{28}$$

with $\alpha_k = (1-2\nu_k)/(2\mu_k(1-\nu_k))$ for $k = 0,1,\ldots,n$ and $\beta_0 = (2(4-5\nu_0))/(15\mu_0(1-\nu_0))$.

Using Eqs. (21), (26) and (28), $\boldsymbol{\varepsilon}^{k/J}$ becomes

$$\begin{aligned}\varepsilon^{k/J}_{ij} = &\frac{\Delta\mu_k}{15\mu_0(1-\nu_0)}\Big[(5+5\nu_0)\left(\varepsilon^{\Omega_k}_{ij} + \varepsilon^{\Omega_k}_{qq}\delta_{ij} - \varepsilon^{\Omega_{k-1}}_{ij} - \varepsilon^{\Omega_{k-1}}_{qq}\delta_{ij}\right) \\ &+ 6\rho^J_{k-1}\left(2\varepsilon^{\Omega_{k-1}}_{ij} + \varepsilon^{\Omega_{k-1}}_{qq}\delta_{ij}\right) - 6\rho^J_k\left(2\varepsilon^{\Omega_k}_{ij} + \varepsilon^{\Omega_k}_{qq}\delta_{ij}\right)\Big] \\ &+ \frac{\mu_k(\nu_0-\nu_k)}{\mu_0(1-\nu_0)(1-2\nu_k)}P^k_{ij} + \frac{2\Delta\mu_k}{\mu_0(1-\nu_0)} \\ &\left[\left(\rho^J_k - 1\right)Q^k_{ij} - \left(\rho^J_{k-1} - 1\right)Q^{k-1}_{ij}\right]\end{aligned} \tag{29}$$

hence the following expression of ε^{Ω_J} from Eq. (20):

$$\begin{aligned}\varepsilon^{\Omega_J}_{ij} = &\varepsilon^0_{ij} - \left(\rho^n_J\right)^{3/2}\sum_{k=1}^{J}\phi_k T^{Int/J}_{ijpq}\Delta C^k_{pquv}\varepsilon^k_{uv} - \sum_{k=J+1}^{n}\frac{\mu_k(\nu_0-\nu_k)}{\mu_0(1-\nu_0)(1-2\nu_k)}P^k_{ij} \\ &- \sum_{k=J+1}^{n}\frac{\Delta\mu_k}{15\mu_0(1-\nu_0)}\Big[(5+5\nu_0)\left(\varepsilon^{\Omega_k}_{ij} + \varepsilon^{\Omega_k}_{qq}\delta_{ij} - \varepsilon^{\Omega_{k-1}}_{ij} - \varepsilon^{\Omega_{k-1}}_{qq}\delta_{ij}\right) \\ &- 6\rho^J_k\left(2\varepsilon^{\Omega_k}_{ij} + \varepsilon^{\Omega_k}_{qq}\delta_{ij}\right) + 6\rho^J_{k-1}\left(2\varepsilon^{\Omega_{k-1}}_{ij} + \varepsilon^{\Omega_{k-1}}_{qq}\delta_{ij}\right) \\ &+ 30\left(\rho^J_k - 1\right)Q^k_{ij} - 30\left(\rho^J_{k-1} - 1\right)Q^{k-1}_{ij}\Big]\end{aligned} \tag{30}$$

with $\rho^m_n = (a_m/a_n)^2$. Tensors $\boldsymbol{P}^k$ and $\boldsymbol{Q}^k$ are defined as

$$\begin{aligned}P^k_{ij} &= \frac{1}{4\pi}\int_{V_k}\left(\frac{1}{r}\right)_{,ij}\varepsilon_{pp}(\boldsymbol{r})dV \quad \text{for} \quad k = 2,\ldots,n \\ Q^k_{ij} &= \frac{1}{a_k^2\Omega_k}\int_{\Omega_k}(x_i x_j u_p(\boldsymbol{r}))_{,p}dV \quad \text{for} \quad k = 1,\ldots,n\end{aligned} \tag{31}$$

Calculation of unknown tensors $\boldsymbol{P}^k$ and $\boldsymbol{Q}^k$ implies a complex implement, since the local displacements $\boldsymbol{u}(\boldsymbol{r})$ and strains $\boldsymbol{\varepsilon}(\boldsymbol{r})$ are heterogeneous respectively within each domain Ω_k ($k = 1,\ldots,n$) and each phase V_k ($k = 2,3,\ldots,n$).

Within the context of isotropic elasticity, the formulation is carried out by decomposing the average strain $\boldsymbol{\varepsilon}^k$ inside each phase k ($k = 1,2,\ldots,n$) into spherical ε^k_s and deviatoric $\boldsymbol{e}^k$ parts.

2.2.1. Average spherical strains

From Bonfoh et al. [21], performing some calculations leads to the spherical parts of tensors $\boldsymbol{P}^k$, $\boldsymbol{Q}^k$ and $\boldsymbol{\varepsilon}^{k/J}$:

$$P^k_s = 0, \quad Q^k_s = \varepsilon^{\Omega_k}_s, \quad \varepsilon^{k/J}_s = -\frac{4}{3}\alpha_0\Delta\mu_k(\varepsilon^{\Omega_k}_s - \varepsilon^{\Omega_{k-1}}_s) \tag{32}$$

According to Eq. (32), spherical part $\varepsilon^{\Omega_J}_s$ is deduced from Eq. (20):

$$\begin{aligned}\varepsilon^{\Omega_J}_s = &\varepsilon^0_s - \left(\rho^n_J\right)^{3/2}\alpha_0\sum_{k=1}^{J}\phi_k\Delta\kappa_k\varepsilon^k_s + \frac{4}{3}\alpha_0\sum_{k=J+1}^{n}\Delta\mu_k(\varepsilon^{\Omega_k}_s - \varepsilon^{\Omega_{k-1}}_s) \\ &\text{for } k = 1,2,\ldots,n\end{aligned} \tag{33}$$

Eq. (33) is an exact formula and provides a system of n equations from which the spherical part ε^k_s of the average strain inside each phase 'k' can be specified.

2.2.2. Average deviatoric strains

Using Eq. (30), the deviatoric part $\boldsymbol{e}^{\Omega_J}$ of average strain $\boldsymbol{\varepsilon}^{\Omega_J}$ inside Ω_J reads as

$$\begin{aligned}e^{\Omega_J}_{ij} = &e^0_{ij} - \left(\rho^n_J\right)^{3/2}\beta_0\sum_{k=1}^{J}\phi_k\Delta\mu_k e^k_{ij} - \sum_{k=J+1}^{n}\frac{\mu_k(\nu_0-\nu_k)}{\mu_0(1-\nu_0)(1-2\nu_k)}P^{d/k}_{ij} \\ &- \sum_{k=J+1}^{n}\frac{\Delta\mu_k}{15\mu_0(1-\nu_0)}\Big[\left(5+5\nu_0-12\rho^J_k\right)e^{\Omega_k}_{ij} \\ &- \left(5+5\nu_0-12\rho^J_{k-1}\right)e^{\Omega_{k-1}}_{ij} + 30\left(\rho^J_k - 1\right)Q^{d/k}_{ij} \\ &- 30\left(\rho^J_{k-1} - 1\right)Q^{d/k-1}_{ij}\Big]\end{aligned} \tag{34}$$

where $\boldsymbol{P}^{d/k}$ and $\boldsymbol{Q}^{d/k}$ are respectively the deviatoric parts of $\boldsymbol{P}^k$ and $\boldsymbol{Q}^k$. $\boldsymbol{e}^{\Omega_J}$ cannot be directly evaluated since tensors $\boldsymbol{P}^k$ and $\boldsymbol{Q}^k$ remain to be determined. To overcome this difficulty, these tensors can be expressed from integral terms of local displacements and strain fields provided respectively in Eqs. (6) and (7). In this manner, Eq. (7) allows to rewrite $\boldsymbol{P}^{d/k}$:

$$\begin{aligned}P^{d/k}_{ij} = &\frac{1}{4\pi}\int_{V_k}\left(\frac{1}{r}\right)_{,ij}\varepsilon^0_{qq}dV_k - \frac{1}{4\pi}\sum_{p=1}^{n}\int_{V_p}\left(\int_{V_k}\left(\frac{1}{r}\right)_{,ij}\Gamma_{qquv}(\boldsymbol{r}-\boldsymbol{r}')dV_k\right) \\ &\times\Delta C^p_{uvmo}\varepsilon_{mo}(\boldsymbol{r}')dV'_p\end{aligned} \tag{35}$$

It should be noted that the first integral term in Eq. (35) vanishes. Let us now introduce fourth-order tensors $\boldsymbol{H}^*$:

$$H^*_{ijuv}(r') = \int_{V_k}\left(\frac{1}{r}\right)_{,ij}\Gamma_{qquv}(\boldsymbol{r}-\boldsymbol{r}')dV_k \quad \text{for } * = 1,2,3 \tag{36}$$

$\boldsymbol{r}'$ is the position of the phase 'p' in the composite inclusion Ω_n. To determine the second integral term of Eq. (35), Ω_n is decomposed into three independent volumes: Ω_{k-1} $(0 \leqslant r' \leqslant a_{k-1})$, V_k $(a_{k-1} \leqslant r' \leqslant a_k)$ and $\Omega_n - \Omega_k$ $(a_k \leqslant r' \leqslant a_n)$. Thanks to this decomposition, Eq. (35) can be rewritten as

$$\begin{aligned} P^{d/k}_{ij} = &-\frac{1}{4\pi}\sum_{p=1}^{k-1}\int_{V_p} H^1_{ijuv}(\boldsymbol{r})\Delta C^p_{uvmo}\varepsilon_{mo}(\boldsymbol{r})dV_p \\ &-\frac{1}{4\pi}\int_{V_k} H^2_{ijuv}(\boldsymbol{r})\Delta C^k_{uvmo}\varepsilon_{mo}(\boldsymbol{r})dV_k \\ &-\frac{1}{4\pi}\sum_{p=k+1}^{n}\int_{V_p} H^3_{ijuv}(\boldsymbol{r})\Delta C^p_{uvmo}\varepsilon_{mo}(\boldsymbol{r})dV_p \end{aligned} \tag{37}$$

Based on Fourier's Transform, we can express tensors $\boldsymbol{H}^*$ $(* = 1,2,3)$ as

$$\begin{aligned} H^1_{ijuv}(\boldsymbol{r}) &= \frac{2\alpha_0}{5a^3_{k-1}}\left(\left(\rho^{k-1}_k\right)^{3/2}-1\right)J^2_{ijuv} \\ H^2_{ijuv}(\boldsymbol{r}) &= \frac{\alpha_0}{40\pi a^3_{k-1}}\left(-10\delta_{ij}\varphi^{Ext/k-1}_{,uv}(\boldsymbol{r})+15\psi^{Ext/k-1}_{,ijuv}(\boldsymbol{r})+16\pi\left(\rho^{k-1}_k\right)^{3/2}J^2_{ijuv}\right) \\ H^3_{ijuv}(\boldsymbol{r}) &= -\frac{\alpha_0}{10}\left(a^2_k-a^2_{k-1}\right)\left(\frac{1}{r}\right)_{,ijuv} \end{aligned} \tag{38}$$

After proceeding to some integral calculations, we express tensors $\boldsymbol{P}^{\boldsymbol{d}/k}$ $(k = J+1,\ldots,n)$:

$$\begin{aligned} P^{d/k}_{ij} = &-\frac{4\alpha_k}{15}\left(\left(\rho^J_k\right)^{3/2}-1\right)\sum_{p=1}^{k-1}\Bigg[\Delta\mu_p\left(\left(\rho^p_J\right)^{3/2}-\left(\rho^{p-1}_J\right)^{3/2}\right)e^p_{ij} \\ &-\frac{4\alpha_k}{15}\Delta\mu_k\left(\left(1-\rho^J_k\right)\left(6e^{\Omega_k}_{ij}-15Q^{d/k}_{ij}+15Q^{d/k-1}_{ij}\right)\right. \\ &\left.+\left(6\rho^J_{k-1}-5-\rho^{k-1}_k\right)e^{\Omega_{k-1}}_{ij}\right)\Bigg]+\frac{4\alpha_k}{5}\left(1-\rho^{k-1}_k\right) \\ &\times\sum_{p=k+1}^{n}\Delta\mu_p\left(-2\rho^k_p e^{\Omega_p}_{ij}+2\rho^k_{p-1}e^{\Omega_{p-1}}_{ij}+5\rho^k_p Q^{d/p}_{ij}-5\rho^k_{p-1}Q^{d/p-1}_{ij}\right) \end{aligned} \tag{39}$$

By executing the same procedure as the latter one from Eqs. (37)–(39), we can also determine the tensor $\boldsymbol{Q}^{\boldsymbol{k}}$ defined in Eq. (31). The overall volume Ω_n is thus decomposed into Ω_k $(0 \leqslant r' \leqslant a_k)$ and $\Omega_n - \Omega_k$ $(a_k \leqslant r' \leqslant a_n)$. $\boldsymbol{Q}^{\boldsymbol{k}}$ becomes

$$\begin{aligned} Q^k_{ij} = &\frac{2}{5}e^0_{ij}+\frac{1}{a^2_k\Omega_k}\sum_{p=1}^{k}\int_{V_p}K^1_{ijuv}(\boldsymbol{r}')\Delta C^p_{uvmo}\varepsilon_{mo}(\boldsymbol{r}')dV'_p \\ &+\frac{1}{a^2_k\Omega_k}\sum_{p=k+1}^{n}\int_{V_p}K^2_{ijuv}(\boldsymbol{r}')\Delta C^p_{uvmo}\varepsilon_{mo}(\boldsymbol{r}')dV'_p \end{aligned} \tag{40}$$

$$\text{with} \quad K^*_{ijuv}(\boldsymbol{r}') = \int_{\Omega_k}\left(x_i x_j G_{qu,v}(\boldsymbol{r}-\boldsymbol{r}')\right)_{,q}dV_k \quad \text{for } * = 1,2 \tag{41}$$

Fourier's Transform technique allows to explicit tensors $\boldsymbol{K}^*$:

$$\begin{aligned} K^1_{ijuv}(\boldsymbol{r}) = &\frac{1}{105\mu_0}\left[(3r^2-7a^2_k)A_{ijuv}-15B_{ijuv}\right. \\ &\left.+21(\delta_{ij}x_u x_v+\delta_{iu}x_j x_v+\delta_{ju}x_i x_v)\right] \\ &-\frac{1}{420\mu_0(1-\nu_0)}\left[-105a^2_k J^1_{ijuv}+(7a^2_k-9r^2)A_{ijuv}\right. \\ &\left.-18B_{ijuv}+21(r^2\delta_{uv}+2x_u x_v)\delta_{ij}\right] \end{aligned} \tag{42}$$

$$\begin{aligned} K^2_{ijuv}(\boldsymbol{r}) = &\frac{a^5_k}{15\mu_0}\left(\delta_{iu}\left(\frac{1}{r}\right)_{,jv}+\delta_{ju}\left(\frac{1}{r}\right)_{,iv}+\alpha_0\left(\frac{1}{r}\right)_{,uv}\delta_{ij}\right) \\ &-\frac{\nu_0 a^7_k}{105\mu_0(1-\nu_0)}\left(\frac{1}{r}\right)_{,ijuv}-\frac{a^5_k}{30\mu_0(1-\nu_0)}r_{,ijuv} \end{aligned}$$

In each phase $k = 1,2,\ldots,n$, $\boldsymbol{Q}^{\boldsymbol{d}/\boldsymbol{k}}$ therefore reads as

$$\begin{aligned} Q^{d/k}_{ij} = &\frac{2}{5}e^0_{ij}+\sum_{p=1}^{k}\left(-\frac{3}{5}\alpha_0\left(\rho^p_k\right)^{5/2}\Delta\lambda_p R^{d/p}_{ij}+2\Delta\mu_p A^p_{ij}\right) \\ &+\sum_{p=k+1}^{n}\left(\frac{2}{5}\alpha_0\Delta\lambda_p P^{d/p}_{ij}+2\Delta\mu_p B^p_{ij}\right) \end{aligned} \tag{43}$$

with $\Delta\lambda_p = \lambda_p - \lambda_0, \lambda_k = 2\mu_k\,\nu_k/(1-2\nu_k)$ for $k = 0,1,\ldots,n$ and

$$\begin{aligned} A^p_{ij} = &\frac{1}{210\mu_0}\Bigg[-6\left(\rho^p_k\right)^{5/2}e^{\Omega_p}_{ij}+6\left(\rho^{p-1}_k\right)^{5/2}e^{\Omega_{p-1}}_{ij} \\ &-28\left(\left(\rho^p_k\right)^{3/2}-\left(\rho^{p-1}_k\right)^{3/2}\right)e^p_{ij}-15\left(\rho^{p-1}_k\right)^{5/2}Q^{d/p-1}_{ij} \\ &+15\left(\rho^p_k\right)^{5/2}Q^{d/p}_{ij}-63\left(\rho^p_k\right)^{5/2}R^{d/p}_{ij}\Bigg] \\ &-\frac{1}{210\mu_0(1-\nu_0)}\Bigg[7\left(\left(\rho^p_k\right)^{3/2}-\left(\rho^{p-1}_k\right)^{3/2}\right)e^p_{ij} \\ &-27\left(\rho^p_k\right)^{5/2}e^{\Omega_p}_{ij}+27\left(\rho^{p-1}_k\right)^{5/2}e^{\Omega_{p-1}}_{ij}-36\left(\rho^{p-1}_k\right)^{5/2}Q^{d/p-1}_{ij} \\ &+36\left(\rho^p_k\right)^{5/2}Q^{d/p}_{ij}-63\left(\rho^p_k\right)^{5/2}R^{d/p}_{ij}\Bigg] \end{aligned} \tag{44}$$

$$\begin{aligned} B^p_{ij} = &\frac{1}{15\mu_0}\left(e^{\Omega_p}_{ij}-e^{\Omega_{p-1}}_{ij}\right) \\ &-\frac{4\nu_0}{35\mu_0(1-\nu_0)}\left(-2\rho^k_p e^{\Omega_p}_{ij}+2\rho^k_{p-1}e^{\Omega_{p-1}}_{ij}+5\rho^k_p Q^{d/p}_{ij}-5\rho^k_{p-1}Q^{d/p-1}_{ij}\right) \\ &-\frac{1}{15\mu_0(1-\nu_0)}\left(2e^{\Omega_p}_{ij}-2e^{\Omega_{p-1}}_{ij}+6Q^{d/p-1}_{ij}-6Q^{d/p}_{ij}+3\nu_0 P^{d/p}_{ij}\right) \end{aligned}$$

Eqs. (43) and (44) highlight a supplementary unknown tensor $\boldsymbol{R}^{\boldsymbol{k}}$:

$$R^k_{ij} = \frac{1}{a^2_k\Omega_k}\int_{V_k}x_i x_j\varepsilon_{pp}dV_k \tag{45}$$

In order to explicit deviatoric part of tensor $\boldsymbol{R}^{\boldsymbol{k}}$, we now decompose the composite inclusion Ω_n into three independent domains in the same way as to obtain Eq. (37):

$$\begin{aligned} R^k_{ij} = &\frac{1}{a^2_k\Omega_k}\Bigg[\int_{V_k}x_i x_j\varepsilon^0_{pp}dV_k-\sum_{p=1}^{k-1}\int_{V_p}L^1_{ijuv}(\boldsymbol{r}')\Delta C^p_{uvmo}\varepsilon_{mo}(\boldsymbol{r}')dV'_p \\ &-\int_{V_k}L^2_{ijuv}(\boldsymbol{r}')\Delta C^p_{uvmo}\varepsilon_{mo}(\boldsymbol{r}')dV'_k-\sum_{p=k+1}^{n}\int_{V_p}L^3_{ijuv}(\boldsymbol{r}')\Delta C^p_{uvmo}\varepsilon_{mo}(\boldsymbol{r}')dV'_p\Bigg] \end{aligned} \tag{46}$$

with $L^*_{ijkl} = \int_{V_k}x_i x_j\Gamma_{ppkl}(\boldsymbol{r}-\boldsymbol{r}')dV_k$ for $* = 1,2,3$.

Still using Fourier's Transform, tensors $\boldsymbol{L}^*$ are also deduced:

$$\begin{cases} L^1_{ijuv}(\boldsymbol{r}') = -\frac{\alpha_0}{5}\left(a^2_k-a^2_{k-1}\right)J^2_{ijuv} \\ L^2_{ijuv}(\boldsymbol{r}') = \frac{\alpha_0}{105}\left[a^7_{k-1}\left(\frac{1}{r'}\right)_{,ijuv}+7a^5_{k-1}\left(\frac{1}{r'}\right)_{,uv}\delta_{ij}-3\left(5B_{ijuv}-7x_u x_v\delta_{ij}\right.\right. \\ \qquad\qquad \left.\left.+2r'^2J^1_{ijuv}+\left(5r'^2-7a^2_k\right)J^2_{ijuv}\right)\right] \\ L^3_{ijuv}(\boldsymbol{r}') = -\frac{\alpha_0}{105}\left(\left(a^7_k-a^7_{k-1}\right)\left(\frac{1}{r'}\right)_{,ijuv}+7\left(a^5_k-a^5_{k-1}\right)\left(\frac{1}{r'}\right)_{,uv}\delta_{ij}\right) \end{cases} \tag{47}$$

It should be observed that the following integral term is a pure spherical tensor:

$$\int_{V_k}x_i x_j \mathrm{d}V_k = \frac{4\pi}{15}\left(a^5_k-a^5_{k-1}\right)\delta_{ij} \tag{48}$$

According to the latter consideration from Eq. (48), the deviatoric part $\boldsymbol{R^{d/k}}$ ($k = 1,2,\ldots,n$) can be formulated as

$$\begin{aligned} R_{ij}^{d/k} = & \frac{2\alpha_k}{5}\left(1-\rho_k^{k-1}\right)\sum_{p=1}^{k-1}\Delta\mu_p\left(\left(\rho_k^p\right)^{3/2}-\left(\rho_k^{p-1}\right)^{3/2}\right)e_{ij}^p \\ & -\frac{2}{35}\alpha_k\Delta\mu_k\left[8\left(1-\left(\rho_k^{k-1}\right)^{7/2}\right)e_{ij}^{\Omega_k}+7\left(\rho_k^{k-1}\right)^{3/2}\left(1-\rho_k^{k-1}\right)e_{ij}^{\Omega_{k-1}}\right. \\ & \left.-20\left(1-\left(\rho_k^{k-1}\right)^{7/2}\right)Q_{ij}^{d/k}\right]+\frac{8\alpha_k}{35}\left(1-\left(\rho_k^{k-1}\right)^{7/2}\right) \\ & \times\sum_{p=k+1}^{n}\Delta\mu_p\left(-2\rho_p^k e_{ij}^{\Omega_p}+2\rho_{p-1}^k e_{ij}^{\Omega_{p-1}}+5\rho_p^k Q_{ij}^{d/p}-5\rho_{p-1}^k Q_{ij}^{d/p-1}\right) \end{aligned} \tag{49}$$

From expressions (39), (43) and (49) respectively of tensors $\boldsymbol{P^{d/k}}$, $\boldsymbol{Q^{d/k}}$ and $\boldsymbol{R^{d/k}}$, developing Eq. (34) for $J = 1,\ldots,n$ provides a system of n equations from which we determine the deviatoric part of strain field inside each of the n phases of the composite inclusion, knowing the imposed deviatoric strain $\boldsymbol{e^0}$.

In the next part, concentration relations obtained from the strain localisation are used to predict the effective elastic properties of composite materials with multi-coated spherical inclusions. These effective properties are evaluated according to a homogenisation method based on the GSCS.

2.3. (n + 1)-Phase self-consistent model

The GSCS is a homogenisation scheme initially developed by Christensen and Lo [7] for the estimation of effective properties of two-phase materials called the '(2 + 1)-phase' self-consistent model. According to the model, the material consists of an inclusion coated by the matrix set as the layer and embedded in an infinite medium having the elastic properties of the homogeneous equivalent medium (HEM). This model is extended to the '(n + 1)-phase' model (see [8,9]).

As shown by Fig. 1, the materials are modelled by an inclusion '*1*' with elastic moduli $\boldsymbol{C^1}$, surrounded by $n-2$ coating layers with elastic moduli $\boldsymbol{C^k}$ ($k = 2,\ldots,n-1$) and placed in a matrix 'n' with elastic moduli $\boldsymbol{C^n}$. The fictitious phase '$n+1$' considered in the scheme designates the HEM, which corresponds to the reference medium '*0*' ($\boldsymbol{C^{n+1}} = \boldsymbol{C^0}$).

From the localisation Eqs. (33) and (34), the GSCS is performed to estimate the effective elastic moduli $\boldsymbol{C^{eff}}$ of the HEM. When the composite material is subjected to a homogeneous displacement $u_i^0 = E_{ij}x_j$ at boundaries, averaging the local strain and stress fields over V respectively leads to uniform macroscopic fields $\boldsymbol{E}$ and $\boldsymbol{\Sigma}$:

$$E_{ij} = \frac{1}{V}\int_V \varepsilon_{ij}(\mathbf{r})dV = \sum_{k=1}^{n} f_k\varepsilon_{ij}^k, \quad \Sigma_{ij} = \frac{1}{V}\int_V \sigma_{ij}(\mathbf{r})dV = \sum_{k=1}^{n} f_k\sigma_{ij}^k \tag{50}$$

where f_k denotes the volume fraction of each phase k ($k = 1,\ldots,n$).

The macroscopic fields are then used to define the effective elastic behaviour:

$$\Sigma_{ij} = C_{ijpq}^{eff}E_{pq} \tag{51}$$

According to the intrinsic assumption of self-consistent scheme, replacing strain $\boldsymbol{\varepsilon^0}$ and moduli $\boldsymbol{C^0}$ in concentration Eqs. (33) and (34) respectively by $\boldsymbol{E}$ and $\boldsymbol{C^{eff}}$ yields

$$\varepsilon_s^{\Omega_J} = E_S - \left(\rho_J^n\right)^{3/2}\alpha_{eff}\sum_{k=1}^{J} f_k\Delta\kappa_k\varepsilon_s^k + \frac{4}{3}\alpha_{eff}\sum_{k=J+1}^{n}\Delta\mu_k\left(\varepsilon_s^{\Omega_k}-\varepsilon_s^{\Omega_{k-1}}\right)$$

$$\begin{aligned} e_{ij}^{\Omega_J} = & E_{ij}^d - \left(\rho_J^n\right)^{3/2}\beta_{eff}\sum_{k=1}^{J} f_k\Delta\mu_k e_{ij}^k - \sum_{k=J+1}^{n}\frac{\mu_k(\nu_{eff}-\nu_k)}{\mu_{eff}(1-\nu_{eff})(1-2\nu_k)}P_{ij}^{ed/k} \\ & -\sum_{k=J+1}^{n}\frac{\Delta\mu_k}{15\mu_{eff}(1-\nu_{eff})}\left[\left(5+5\nu_{eff}-12\rho_k^J\right)e_{ij}^{\Omega_k}\right. \\ & -\left(5+5\nu_{eff}-12\rho_{k-1}^J\right)e_{ij}^{\Omega_{k-1}}+30\left(\rho_k^J-1\right)Q_{ij}^{ed/k} \\ & \left.-30\left(\rho_{k-1}^J-1\right)Q_{ij}^{ed/k-1}\right] \end{aligned} \tag{52}$$

where $\Delta\kappa_k = \kappa_k - \kappa_{eff}$, $\Delta\mu_k = \mu_k - \mu_{eff}$. Still from self-consistent assumption, we also define scalars α_{eff}, β_{eff} by replacing subscript '0' (reference medium) by '*eff*' (HEM). Tensors $P_{ij}^{ed/k}$, $Q_{ij}^{ed/k}$ are deduced from Eqs. (39), (43) and (49).

The system of Eq. (52) for $J = 1,2,\ldots,n$ provides the average strain $\boldsymbol{\varepsilon^k}$ in each phase 'k' of the composite inclusion as a function of the macroscopic strain $\boldsymbol{E}$:

$$\varepsilon_{ij}^k = A_{ijpq}^k E_{pq} \quad \text{for } k = 1,2,\ldots,n \tag{53}$$

where $\boldsymbol{A^k}$ is the strain localisation tensor of the phase 'k'.

Using Eqs. (50), (51) and (53) allow to obtain

$$C_{ijpq}^{eff} = C_{ijpq}^n + \sum_{k=1}^{n-1} f_k\left(C_{iju\nu}^k - C_{iju\nu}^n\right)A_{u\nu pq}^k \tag{54}$$

From Eq. (54), the isotropic property of elastic moduli tensors leads to

$$\begin{aligned} \mu_{eff} &= \mu_n + \sum_{k=1}^{n-1} f_k(\mu_k-\mu_n)A_d^k \\ \kappa_{eff} &= \kappa_n + \sum_{k=1}^{n-1} f_k(\kappa_k-\kappa_n)A_s^k \end{aligned} \tag{55}$$

In Eq. (55), we can note that the evaluation of $\boldsymbol{C^{eff}}$ only requires calculation of the spherical part A_s^k and deviatoric part A_d^k of $\boldsymbol{A^k}$. The latter terms are determined using Eqs. (52) and (53).

It should be emphasised that the solution of multi-coated inclusion problem is acquired for an arbitrary number of coatings. This achievement is rigorous without any restrictive assumption and provides analytical concentration equations. Performing then the GSCS enables to predict the local stress and strain fields in each phase and the effective behaviour of the composite material.

In the next section, the general analytical solution is applied to predict the effective behaviour of the three-phase composite material.

3. Application to three-phase materials with homothetic spherical inclusions

In this section, the model is applied to the particular case of a three-phase composite material. In this case, the '(3 + 1)-phase' model is performed. Spherical parts of local strain fields are deduced from Eq. (52):

$$\begin{aligned} A_s^1 &= \frac{(f_1+f_2)(3\kappa_{eff}+4\mu_{eff})(3\kappa_2+4\mu_2)(3\kappa_3+4\mu_3)}{\Delta} \\ A_s^2 &= \frac{(f_1+f_2)(3\kappa_{eff}+4\mu_{eff})(3\kappa_1+4\mu_2)(3\kappa_3+4\mu_3)}{\Delta} \\ A_s^3 &= \frac{(3\kappa_{eff}+4\mu_{eff})[12f_1(\kappa_1-\kappa_2)(\mu_2-\mu_3)+(f_1+f_2)(3\kappa_1+4\mu_2)(3\kappa_2+4\mu_3)]}{\Delta} \end{aligned} \tag{56}$$

with:

$$\begin{aligned} \Delta = & 12(f_1+f_2)^2(\kappa_2-\kappa_3)(3\kappa_1+4\mu_2)(\mu_3-\mu_{eff}) + 12f_1(\kappa_1-\kappa_2) \\ & \times(3\kappa_3+4\mu_{eff})(\mu_2-\mu_3) + (f_1+f_2)[12f_1(\kappa_1-\kappa_2)(3\kappa_3+4\mu_2) \\ & \times(\mu_3-\mu_{eff}) + (3\kappa_1+4\mu_2)(3\kappa_2+4\mu_3)(3\kappa_3+4\mu_{eff})] \end{aligned}$$

Applying the deviatoric parts of local strain fields expressed in Eq. (52) to the '(3 + 1)-phase' model enables to obtain a system of three equations:

$$\begin{aligned} e_{ij}^{\Omega_J} = & E_{ij}^d - \left(\rho_J^3\right)^{3/2}\beta_{eff}\sum_{k=1}^{J} f_k(\mu_k-\mu_{eff})e_{ij}^k \\ & -\sum_{k=J+1}^{3}\frac{\mu_k(\nu_{eff}-\nu_k)}{\mu_{eff}(1-\nu_{eff})(1-2\nu_k)}P_{ij}^{ed/k} \\ & -\sum_{k=J+1}^{3}\frac{(\mu_k-\mu_{eff})}{15\mu_{eff}(1-\nu_{eff})}\left[\left(5+5\nu_{eff}-12\rho_k^J\right)e_{ij}^{\Omega_k}\right. \\ & -\left(5+5\nu_{eff}-12\rho_{k-1}^J\right)e_{ij}^{\Omega_{k-1}}+30\left(\rho_k^J-1\right)Q_{ij}^{ed/k} \\ & \left.-30\left(\rho_{k-1}^J-1\right)Q_{ij}^{ed/k-1}\right] \quad \text{for } J = 1,2,3 \end{aligned} \tag{57}$$

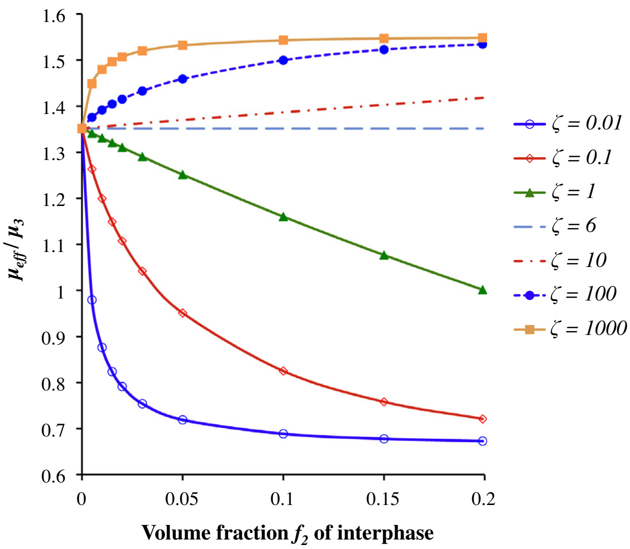

Fig. 2. Normalised effective shear modulus μ_{eff}/μ_3 versus volume fraction f_2 of the interphase for different values of $\zeta = \mu_2/\mu_3$ from 0.01 to 1000. $\nu_1 = \nu_2 = \nu_3 = 0.3$ and $f_1 + f_2 = 0.2$.

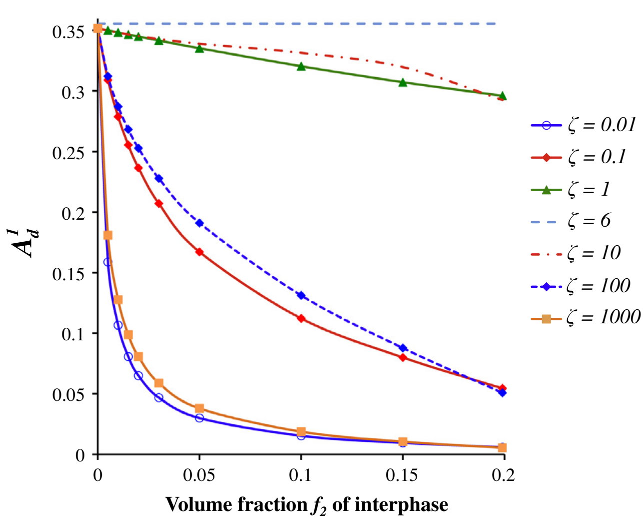

Fig. 3. Deviatoric part of strain localisation tensor A_d^1 in the inclusion (phase '1') versus volume fraction f_2 of the interphase for different values of $\zeta = \mu_2/\mu_3$ from 0.01 to 1000. $\nu_1 = \nu_2 = \nu_3 = 0.3$ and $f_1 + f_2 = 0.2$.

According to this model, Eqs. (39), (43) and (49) provide a system of 8 equations from which we can deduce the expressions of effective tensors $\boldsymbol{P}^{d/k}$ (for $k = 2,3$), $\boldsymbol{Q}^{d/k}$ (for $k = 1,2,3$) and $\boldsymbol{R}^{d/k}$ (for $k = 1,2,3$). After substituting the latter expressions in the system of equations defined in Eq. (57), we proceed to the system solving by using the formal calculation software 'Wolfram Mathematica'. Therefore, we achieve the evaluation of the local deviatoric strain fields of the three considered phases:

$$e_{ij}^k = A_d^k E_{ij}^d \quad \text{for } k = 1,2,3 \tag{58}$$

To verify the accuracy of the present model, the obtained results are compared with the exact solution and some outcomes of numerical investigations.

3.1. Comparison with the exact solution

First, it is important to note that strain concentration relations obtained in this work correspond exactly to those deduced from the approach suggested by Hervé and Zaoui [8]. The general analytical expressions of localisation tensors are then implemented for the estimation of the effective properties of a composite material using GSCS. In Fig. 2, all curves of the normalised effective shear modulus versus the volume fraction f_2 of the interphase strictly coincide with those of Hervé and Zaoui's model [8], whatever the value of the parameter $\zeta = \mu_2/\mu_3$. The results displayed in Fig. 2 thus allow to verify that the proposed model leads to the exact solution of the multi-coated inclusion problem.

Figs. 3 and 4 show the dependence of the deviatoric part of strain localisation tensors on the interphase volume fraction f_2, respectively inside the inclusion A_d^1 and the matrix A_d^3. Since the volume fraction of the composite inclusion $f_1 + f_2$ is constant and equal to *0.2* in this case, A_d^1 and A_d^3 versus f_2 also remain constant for $\zeta = 6(\mu_2 = \mu_1 = 6\mu_3)$. When the interphase material is set to be softer than the matrix ($\zeta < 6$), A_d^3 decreases with f_2. Due to the condition $\mu_2 < \mu_1$ and $\mu_1 = 6\ \mu_3$, A_d^1 follows a similar trend to A_d^3 when $\zeta < 6$. On the other hand, when the interphase is more rigid than

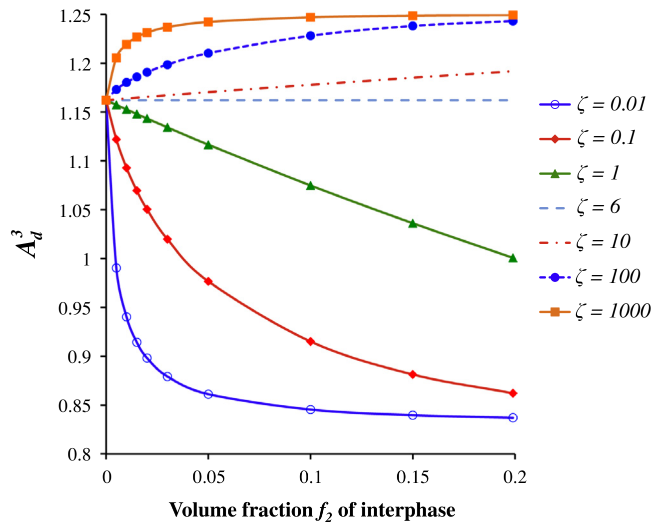

Fig. 4. Deviatoric part of strain localisation tensor A_d^3 in the matrix (phase '3') versus volume fraction f_2 of the interphase for different values of $\zeta = \mu_2/\mu_3$ from 0.01 to 1000. $\nu_1 = \nu_2 = \nu_3 = 0.3$ and $f_1 + f_2 = 0.2$.

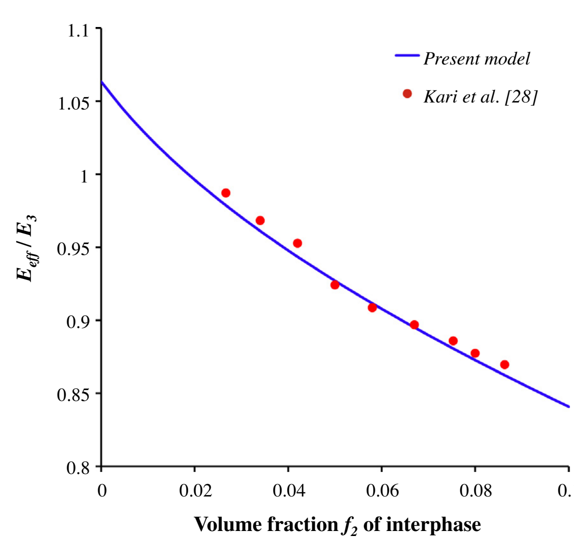

Fig. 5. Normalised effective Young modulus E_{eff}/E_3 versus volume fraction f_2 of interphase for a volume fraction of inclusion $f_1 = 0.15$.

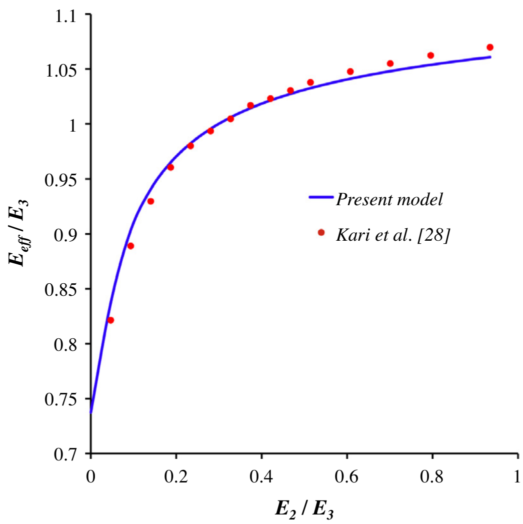

Fig. 6. Normalised effective Young modulus E_{eff}/E_3 versus normalised Young modulus E_2/E_3 of interphase for volume fractions of inclusion $f_1 = 0.15$ and interphase $f_2 = 0.0378$.

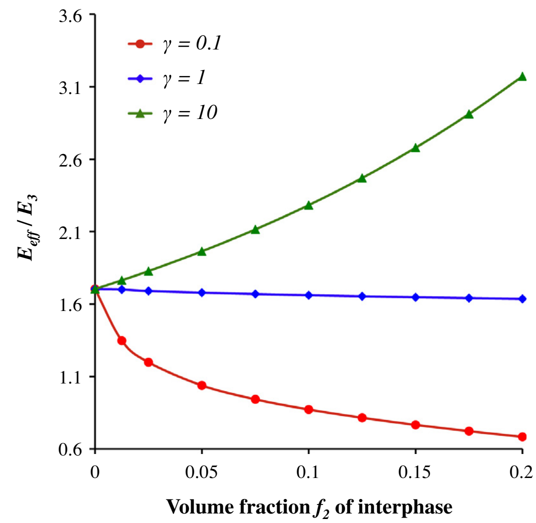

Fig. 8. Normalised effective Young modulus E_{eff}/E_3 versus volume fraction f_2 of the interphase for three values of $\gamma = E_2/E_3$ (0.1, 1, 10). $\nu_1 = 0.2, \nu_2 = 0.3$, $\nu_3 = 0.499$ and $f_1 + f_2 = 0.2$.

Table 1
Properties of the three-phase composite material used for applications and comparison with numerical model of Kari et al. [28].

Material	Young's modulus (GPa)	Poisson's ratio
Particle (tungsten)	$E_1 = 345$	$\nu_1 = 0.28$
Interphase (carbon)	$E_2 = 34.48$	$\nu_2 = 0.2$
Matrix (nickel)	$E_3 = 214$	$\nu_3 = 0.31$

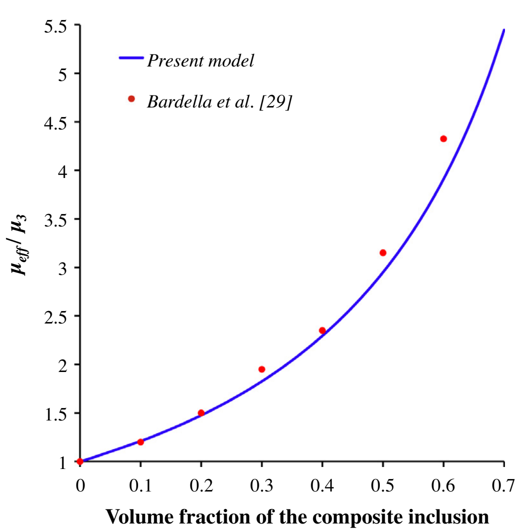

Fig. 7. Normalised effective shear modulus μ_{eff}/μ_3 versus volume fraction of the composite inclusion ($f_1 + f_2$).

the core ($\zeta > 6$), A_d^1 still decreases with f_2 while A_d^3 is driven by an opposite trend and increases with respect to f_2. We also note that A_d^3 varies much more sensitively with the ratio ζ when the interphase is softer than the matrix. Consequently, manufacturing composite materials seems to be more efficient with softer coating layers to increase damping than with stiffer ones to improve stiffening.

Besides, spherical local strains are explicitly given by analytical expressions (see Eq. (56)).

Finally, setting $\boldsymbol{C}^1$ equal to $\boldsymbol{C}^2$ from the localisation equations above leads to the '(2 + 1)-phase' model and provides results that match those of Bonfoh et al.'s initial model [21].

3.2. Applications and comparison with numerical models

For further examination, predictions of the effective properties of a three-phase composite material are given through comparisons between the present model and numerical achievements. In Figs. 5 and 6, the results concern the comparison with Kari et al.'s investigation [27], for which material properties considered are listed in Table 1. Kari et al.'s results [27] have been obtained through numerical homogenisation techniques based on the FEM. Fig. 5 illustrates predictive curves regarding the effective Young's modulus dependency on f_2. A good agreement is observed between the curves of both models for a range of f_2 from 0.01 to 0.1.

Since the interphase is softer than the inclusion and the matrix, increasing f_2 leads to a decrease of the effective Young's modulus. Indeed, by increasing f_2 from 0.01 to 0.1, the normalised effective Young's modulus drops from 1.027 to 0.84. The interphase thus seems to significantly influence the effective behaviour of composite material.

Fig. 6 shows the evolution of the effective Young's modulus with respect to the interphase Young's modulus in terms of normalised values. A good agreement is also noted between the present model and Kari et al.'s one [27]. Even for a small value of f_2 (e.g. 0.0378), the effective Young's modulus is enhanced by increasing the ratio E_2/E_3.

By presenting a critical analysis of different micromechanical approaches, Bardella et al. [28] propose a numerical finite-element prediction of the effective elastic properties of composite materials in the case of syntactic foam. Fig. 7 displays the dependence of normalised effective shear modulus on the volume fraction of composite inclusion, according to the present model and the computer implement FEM of Bardella et al. [28]. Predictions of both models appear to be in good agreement with each other.

3.3. Influence of the interphase characteristics

This section is devoted to an in-depth examination of the effective elastic modulus E_{eff} dependence on the volume fraction f_2 and the Young modulus E_2 of the interphase. In this last study, f_2 and E_2

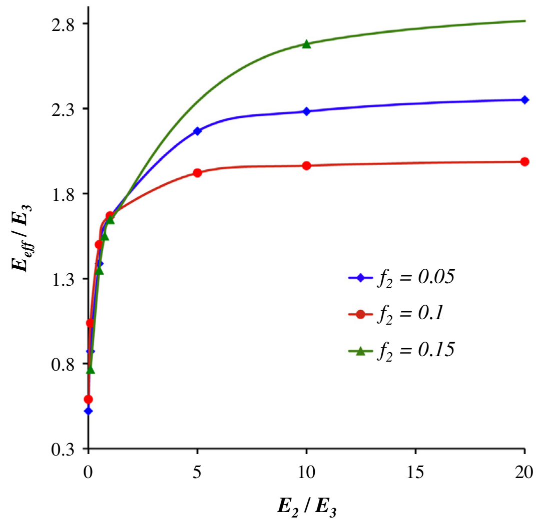

Fig. 9. Normalised effective Young modulus E_{eff}/E_3 versus normalised Young modulus E_2/E_3 of the interphase for three values of f_2 (0.05, 0.1, 0.15). $E_1/E_3 = 100$, $\nu_1 = 0.2$, $\nu_2 = 0.3$, $\nu_3 = 0.499$ and $f_1 + f_2 = 0.2$.

are selected in order to emphasise how they can enhance the overall behaviour of corresponding coated inclusion composite. In this study, the normalised Young modulus of inclusion E_1/E_3 is taken to be 100, while parameter $\gamma = E_2/E_3$ defines that of the coating layer (interphase). Fig. 8 provides the normalised effective Young modulus E_{eff}/E_3 versus f_2. For γ taken from 0.1 up to 1, it is noticeable that E_{eff}/E_3 decreases with f_2. On the other side, from γ set quite above 1, the equivalent properties are significantly improved by the presence of the interphase material, as it is shown when γ is equal to 10. E_{eff}/E_3 versus γ curves displayed in Fig. 9 confirm the latter observations. Indeed, we can clearly observe that from $\gamma > 1$, increasing the volume fraction f_2 between 0.05 and 0.15 results in an enhancement of the effective elastic properties E_{eff}/E_3.

These last results thus provide the extent to which a judicious choice of the interphase material could reinforce a coated inclusion composite.

4. Conclusion

In this paper, we propose a new achievement of the '$(n+1)$-phase' GSCS to predict the effective properties of elastic composite materials with multi-coated reinforcements. The topology of the problem is described by a n-phase multi-coated composite inclusion embedded in an infinite reference medium. Based on the integral equation and thanks to the interior and exterior-point Eshelby's tensors, a general micromechanical formulation of the multi-coated inclusion problem is achieved in the general case of ellipsoidal inclusions and anisotropic elasticity. In order to examine the relevance of the proposed approach, the present model has been performed in isotropic elasticity and spherical multi-coated inclusions. Analytical development provides the expressions of local averaged strains inside inclusion and each coating layer. These analytical results match the exact solution of Hervé and Zaoui [8]. The strain concentration relations are then applied to a three-phase composite material. The accuracy of the obtained '(3 + 1)-phase' model is verified by comparison with numerical results based on FEM. Thereafter, the latter model is used to describe the influence of the interphase between inclusions and matrix on the effective behaviour of the composite material. The resulting curves show that interphase characteristics have a significant influence on the effective behaviour.

Although the only specific resolution of isotropic multi-coated spherical inclusion problem is performed in this work, extending the achievement to the general case of anisotropic and ellipsoidal composite inclusion does not point out any tricky substantial contribution, since no further micromechanical consideration is needed. This generalisation remains a challenging task and the main prospect of this promising method.

References

[1] Gao SL, Mäder E. Characterisation of interphase nanoscale property variations in glass fibre reinforced polypropylene and epoxy resin composites. Compos Part A: Appl Sci Manuf 2002;33(4):559–76.
[2] Torralba JM, Velasco F, Costa CE, Vergara I, Cáceres D. Mechanical behaviour of the interphase between matrix and reinforcement of Al 2014 matrix composite reinforced with $(Ni_3Al)_p$. Compos Part A: Appl Sci Manuf 2002;33(3):427–34.
[3] George SC, Thomas S. Transport phenomena through polymeric systems. Progr Polym Sci 2001;26(6):985–1017.
[4] Eshelby JD. The determination of the elastic field of an ellipsoidal inclusion, and related problems. Proc R Soc Lond A 1957;241(1226):376–96.
[5] Love AEH. A treatise on the mathematical theory of elasticity. 4th ed. MI: Cambridge University Press; 1927.
[6] Hashin Z. The elastic moduli of heterogeneous materials. J Appl Mech 1962;29(1):143–50.
[7] Christensen RM, Lo KH. Solutions for effective shear properties in three phase sphere and cylinder models. J Mech Phys Solids 1979;27(4):315–30.
[8] Hervé E, Zaoui A. n-Layered inclusion-based micromechanical modelling. Int J Eng Sci 1993;31(1):1–10.
[9] Hervé E, Zaoui A. Elastic behaviour of multiply coated fibre-reinforced composites. Int J Eng Sci 1995;33(10):1419–33.
[10] Jasiuk I, Kouider MW. The effect of an inhomogeneous interphase on the elastic constants of transversely isotropic composites. Mech Mater 1993;15(1):53–63.
[11] Huang JS, Gibson LJ. Elastic moduli of a composite of hollow spheres in a matrix. J Mech Phys Solids 1993;41(1):55–75.
[12] Hashin Z, Monteiro PJM. An inverse method to determine the elastic properties of the interphase between the aggregate and the cement paste. Cem Concr Res 2002;32(8):1291–300.
[13] Pensée V, He QC. Generalized self-consistent estimation of the apparent isotropic elastic moduli and minimum representative volume element size of heterogeneous media. Int J Solids Struct 2007;44(7–8):2225–43.
[14] Maligno AR, Warrior NA, Long AC. Effects of interphase material properties in unidirectional fibre reinforced composites. Compos Sci Technol 2010;70(1):36–44.
[15] Rodríguez-Ramos R, Medeiros R, Guinovart-Díaz R, Bravo-Castillero J, Otero JA, Tita V. Different approaches for calculating the effective elastic properties in composite materials under imperfect contact adherence. Compos Struct 2013;99:264–75.
[16] Shokrieh MM, Rafiee R. On the tensile behavior of an embedded carbon nanotube in polymer matrix with non-bonded interphase region. Compos Struct 2010;92(3):647–52.
[17] Shabana YM. A micromechanical model for composites containing multi-layered interphases. Compos Struct 2013;101:265–73.
[18] Hori M, Nemat-Nasser S. Double-inclusion model and overall moduli of multi-phase composites. Mech Mater 1993;14(3):189–206.
[19] Cherkaoui M, Sabar H, Berveiller M. Micromechanical approach of the coated inclusion problem and applications to composite materials. J Eng Mater Technol 1994;116(3):274–8.
[20] Cherkaoui M, Sabar H, Berveiller M. Elastic composites with coated reinforcements: a micromechanical approach for nonhomothetic topology. Int J Eng Sci 1995;33(6):829–43.
[21] Bonfoh N, Hounkpati V, Sabar H. New micromechanical approach of the coated inclusion problem: exact solution and applications. Comput Mater Sci 2012;62:175–83.
[22] Dederichs PH, Zeller R. Variational treatment of the elastic constants of disordered materials. Z Phys 1973;259(2):103–16.
[23] Kröner E. Elastic moduli of perfectly disordered composite materials. J Mech Phys Solids 1967;15(5):319–29.
[24] Eshelby JD. The elastic field outside an ellipsoidal inclusion. Proc R Soc Lond A 1959;252(1271):561–9.
[25] Mura T. Micromechanics of defects in solids. 2nd ed. MI: Martinus Nijhoff Publishers; 1987.
[26] Kröner E. Modified Green function in the theory of heterogeneous and/or anisotropic linearly elastic media. In: Weng GJ, Taya M, Abé H, editors. Micromechanics and inhomogeneity. Berlin: Springer; 1990. p. 197–211.
[27] Kari S, Berger H, Gabbert U, Guinovart-Diaz R, Bravo-Castillero J, Rodriguez-Ramos R. Evaluation of influence of interphase material parameters on effective material properties of three phase composites. Compos Sci Technol 2008;68(3–4):684–91.
[28] Bardella L, Sfreddo A, Ventura C, Porfiri M, Gupta N. A critical evaluation of micromechanical models for syntactic foams. Mech Mater 2012;50:53–69.